DETERMINING OPTIMAL SCANNING SPEED FOR LASER SINTERING OF CP75 POLYPROPYLENE POWDER

J. Nsengimana[1], J.G. van der Walt[2], E.H.G. Langner[3] & D.J. de Beer[4]

[1]Department of Mechanical & Mechatronics Engineering, Central University of Technology, Free State, South Africa, jnsengimana@cut.ac.za

[2] Department of Mechanical & Mechatronics Engineering, Central University of Technology, Free State, South Africa, jgvdwalt@cut.ac.za

[3] Department of Chemistry, University of the Free State, South Africa, LangneEH@ufs.ac.za

[4] Centre for Rapid Prototyping and Manufacturing, Central University of Technology, Free State, South Africa, ddebeer@cut.ac.za

ABSTRACT

Polypropylene (PP) is one of the polymeric materials that can be processed through LS and offers a good combination of physical, chemical, mechanical, thermal, and electrical properties with a good strength to weight ratio. The optimal laser scanning speed was determined for LS a commercial CP75 PP powder supplied by Diamond Plastics GmbH. In combination with other process parameters as recommended by the supplier of the powder, scanning speeds ranging from 1481 to 1600 mm/s were found to be optimal for acceptable mechanical properties, surface finish and dimensional accuracy for an EOS P380 LS machine. Elongation at break was however found to be constantly low.

1. INTRODUCTION

Although Laser Sintering (LS) can process a wide range of materials, 95% of LS production processes of prototypes and functional parts that are based on polymers, involves only nylon polyamides PA11 or PA12 [1]. Polypropylene (PP) is currently one of the most commonly used and versatile semi-crystalline thermoplastics in both short and long run applications [2]. With a good strength to weight ratio, PP offers a good combination of physical, chemical, mechanical, thermal, and electrical properties. It is lightweight, resistant to staining, and does not absorb moisture. Traditionally, due to its versatility, good mechanical performance, chemical stability and relative low cost, PP materials are used in injection or rotational moulding in granular or powder form for automotive, consumer goods, sport-leisure products and in the textile industry [3].

Recent research in the development of materials has shown PP to be suitable for processing through the LS process [4]. Using Differential Scanning Calorimetry (DSC) analysis, Fiedler *et al.* [5] conducted a comparative study on the window of sinterability and the degree of crystallinity of nylon polyamide (PA) grades and a series of homopolymer and copolymer polypropylenes. It was found that the window of sinterability of all considered PP grades was in the same range or sometimes even better than the window of sinterability of the PA references. Furthermore,

ISBN 978-0-6398390-0-4

Thermo-Gravimetry Analysis (TGA) proved that, under a nitrogen atmosphere, PP grades had sufficient and better thermal stability than that of the investigated polyamides, meaning that no degradation of PP powder should occur during the LS process. Lexow and Drummer [6] investigated the effect of the addition of 0.1 wt % of Aerosil R8200 flow agent on the flowability and the degree of crystallinity of cryogenically ground PP powder. Two heterophasic propylene-ethylene copolymers PP Moplen EP600V and EP548V produced by Lyondell Basell Industry N.V. were investigated. It was found that, with little effect on the thermal behavior of the powder, although the addition of the flow agents increased the electrostatic charging of the powder, it also improved the flow behavior of the investigated PP grades. An increase in energy density increased the tensile strength and the Young's modulus but decreased slightly elongation at break of the specimen.

Kleinjnen *et al.* [4] studied the effect of the addition of nucleating agents on mechanical properties of PP components manufactured using the LS process. They found that with little effect on the window of sinterability of the powder, the blending of CP22 PP powder supplied by Diamond Plastics with a sorbitol based nucleating agent increased the impact strength of components produced by up to 99% when the energy density was optimized to 12.8 kJ/m^2. Tan *et al.* [7] investigated the mechanical properties of CP22 PP powder on an EOSINT P395 LS machine with a layer thickness of 100 µm and a hatching distance of 0.25 mm within a range of scanning speeds of 300 to 500 mm/s with energy densities varying from 0.400 to 1.360 J/mm^3. On the other hand, scanning speeds of 4500 and 6000 mm/s with energy densities varying from 0.08 to 0.29 J/mm^3 were considered. The achieved highest ultimate tensile strength and Young modulus were 2.5 MPa and 350 MPa respectively. Zhu *et al.* [8] used PP powder from Trial Corporation, Japan to investigate mechanical and microstructural properties of PP test parts manufactured by LS in comparison to their injection moulded counterparts. The used laser powers (p) were 8.25, 11, 13.75 and 16.5 W; scanning speeds (v) of 1500, 2000, 2500 and 3000 mm/s; a layer thickness (t) of 0.15 mm and a fixed hatch distance (h) of 0.2 mm, which was half of the physical diameter of the laser beam (0.4 mm) to ensure overlaps with the previous scan line. They found that with the used laser power, even the minimum value of 8.25 W, was adequate to fully fuse the powder. Under the premise of proper laser powers, scanning speed was found to be the dominant factor affecting the mechanical strength of the laser sintered parts. A maximum tensile strength of 19.9 MPa was obtained at an energy density of 0.0458 J/mm^2 with an optimal parameter combination of p = 13.75 W, v = 1500 mm/s, t = 0.15 mm and h = 0.2 mm. The achieved tensile strength for LS specimens was 20% (19.9 ± 0.5 MPa vs 16.65 ± 0.3 MPa) greater than the tensile strength of their injection moulded counterparts and the tensile modulus of LS was 72% (599.1±14.1 MPa vs 349.1±9.4 MPa) higher than the tensile modulus of IM specimens. This was attributed to the higher degree of crystallinity and existence of gamma-phase in the LS specimens. However, there was a significant difference between the Elongation at Break of LS and injection moulded specimens which were 150 and 650% respectively.

Recently, Diamond Plastics GmbH initiated the commercialization of PP CP 22, PP CP 50, PP CP 60 and PP CP 75 white or grey polypropylene powder grades for the LS process. The powder has an average particle size of 60 µm. Initial tensile tests performed on laser sintered parts using Diamond Plastics CP 75 with process parameters as provided by the supplier produced parts with inferior mechanical properties. Since Zhu *et al.* [8] found scanning speed to be the most influential process parameter for the mechanical strength of the parts, the aim of this study was to investigate the optimal scanning speed for processing PP CP 75 white powder through LS in terms of mechanical properties, dimensional accuracy and surface finish of parts.

2. METHODOLOGY

Diamond Plastics GmbH recommends the following process parameters for PP CP75 on an EOS P390 LS machine under a nitrogen atmosphere: A layer thickness of 150 µm, scanning speed of 1300 mm/s, hatching distance of 0.25 m, laser power of 10 W, building chamber temperature between 158 and 161°C and removal chamber temperature at 130°C. Research for the current study was performed on an older EOS P380 LS machine under a nitrogen atmosphere. A temperature of 158°C was set for the building chamber while the removal chamber temperature was set at 100°C. The energy density (ED) in J/mm^2 was calculated from the commonly known formula

$$ED = \frac{p}{s \times h}$$

where p -laser power in W; s -scanning speed in mm/s and h-hatching distance in mm. SolidWorks software was used to produce the Computer Aided Design (CAD) of the tensile test pieces (according to ISO 527-2). Table 1 summarizes the experimental LS process parameters that was used for producing the test parts.

Table 1: Process parameters for laser sintering tensile test pieces and dimensional accuracy blocks.

Part Designation	Layer thickness t (mm)	Hatching distance h (mm)	Laser power p (W)	Scanning speed s (mm/s)	Energy density ED (J/mm^2)
X2, Y2, Z2	0.150	0.25	10	1481	0.027
X1, Y1, Z1	0.150	0.25	10	1600	0.025
X0, Y0, Z0	0.150	0.25	10	1740	0.023
X-1, Y-1, Z-1	0.150	0.25	10	1905	0.021
X-2, Y-2, Z-2	0.150	0.25	10	2105	0.019

Figure 1a shows the arrangement of the tensile test pieces in their respective directions along with the test blocks built in x-direction. Three corresponding test blocks were produced for each scanning speed for investigation of dimensional accuracy.

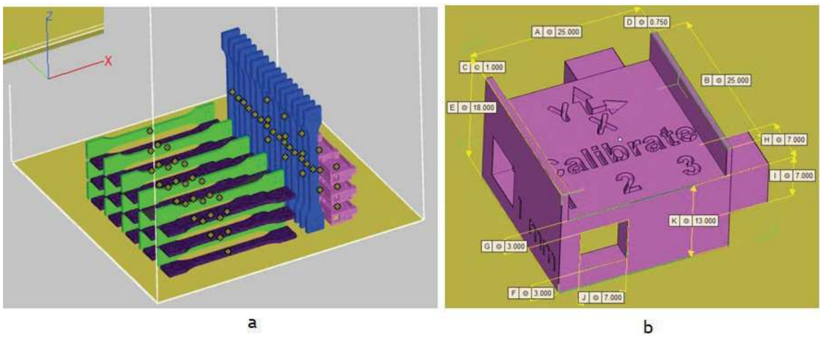

Figure 1: CAD geometry and arrangement of the test pieces in the building chamber (a) and the details of the test block for dimensional accuracy (b)

The design of the test block (Figure 1b) is such that it highlights the weaknesses of the LS process such as thin features and holes and text on vertical surfaces.

ISBN 978-0-6398390-0-4

3. RESULTS AND DISCUSSIONS

3.1. Mechanical properties

The datasheet on laser sintered PP CP75 as provided by Diamond plastics GmbH claims, a tensile strength of 22 MPa, a tensile modulus of 2500 N/mm^2 and an elongation at break of 10% in the x-direction [9]. Initially, under LS process parameters as specified by the supplier of the powder, the tensile test of specimens built in x-direction on the EOS P380 showed a low tensile strength of 14 MPa. The tensile tests were performed according to the ISO 527-2 standard on an MTS Criterion tensile testing machine. In an attempt to improve the measured tensile strength, the scanning speed was reduced to 1000 and 700 mm/s respectively while keeping the other process parameters constant. This however resulted in even lower tensile strengths of 11.9 and 11.4 MPa respectively. To investigate the effect of a progressive increase of the scanning speed on mechanical properties, varying the scanning speed and keeping the other process parameters constant, 45 tensile test pieces were produced in the x, y and z-directions for five scanning speeds greater than the recommended 1300 mm/s scanning speed. Figures 2 a & b show the measured average tensile strength and tensile modulus of each of the specimens built in in the x, y and z-directions.

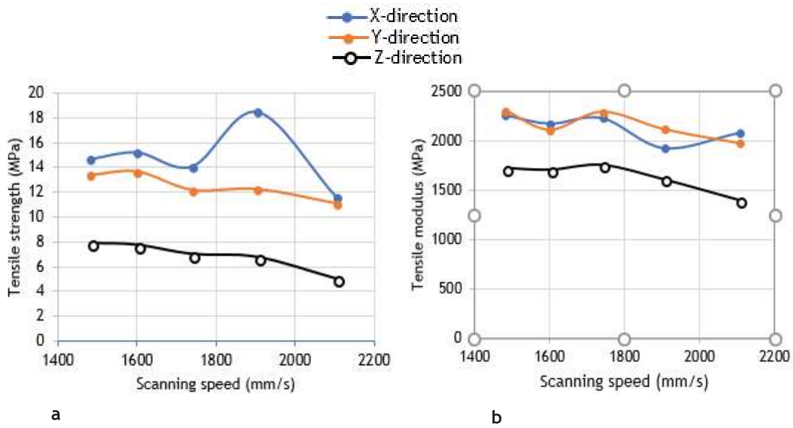

Figure 2: Variation of the tensile strength (a) and the tensile modulus (b) versus the scanning speed

The general trend found was that an increase in the scanning speed leads to a decrease of the tensile strength and the modulus of elasticity of the test pieces. However, in x and y-directions, an increase in tensile strength for scanning speed ranging from 1481 to 1600 mm/s was observed while in z-direction, the tensile strength remains practically unchanged. For a scanning speed of 1905 mm/s, the highest tensile strength of 18.5 MPa was achieved in the x-direction. It was however obvious that this point was far outside the general trend of the curve. Liparoti *et al.* [10] reported that an elastic modulus varying from 1 to 2.9 GPa was obtained for different positions and localizations within injection moulded PP samples. Figure 2b shows that for a scanning speed of 1481 mm/s, moduli of elasticity of 2308, 2294 and 1729 MPa in x, y and z -

directions respectively were obtained. An increase of the scanning speed up to 1740 mm/s resulted in a slight decrease (1%) of the modulus of elasticity in x, y-direction to 2235, 2294 MPa respectively and to a slight increase of 2% in z-direction. It can be concluded that for a scanning speeds ranging from 1481 to 1740 mm/s, the variation of the moduli of elasticity is not significant in the respective directions. Further increase of the scanning speed led to the weakening of the test pieces. The results show that for all scanning speeds, the test pieces built in x-direction exhibit tensile strength and modulus of elasticity higher than the test pieces built in y-direction, which are also stronger than the test pieces built in the z-direction. With ratios varying from 1.04 to 1.15, the differences between tensile strengths in x and y-directions are not very significant whereas there exist significant differences between tensile strengths in x and z-directions where the ratios vary from 1.7 to 2.7.

Porosity was evident in all test pieces as shown by a Scanning Electron Microscope (SEM) image (Figure 3) of the failure surface of a tensile test piece.

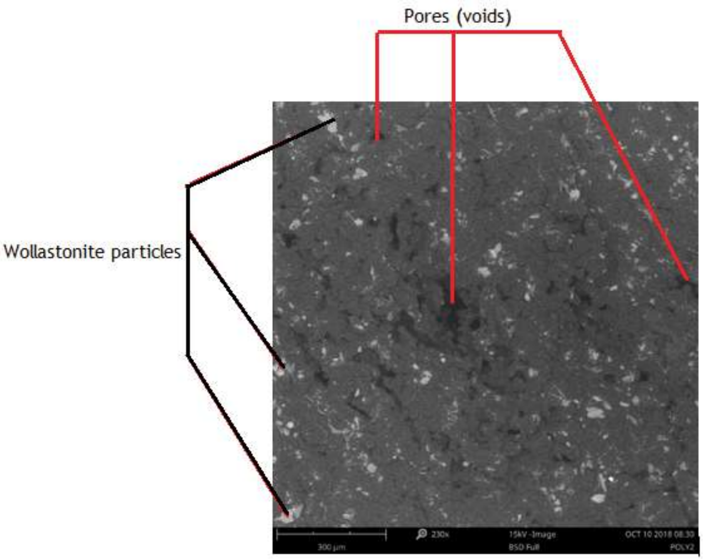

Figure 3: Scanning Electron Microscope image of the failure cross-section of the test piece

This porosity caused a premature failure of the test pieces and producing an elongation at break very close to zero. Abdurashirov and Ob'edkov [11] reported that the addition of wollastonite to polyethylene for the injection moulding process, depending on the added dose, could increase or decrease the tensile strength. An increase of the percentage weight of the wollastonite filler led to a constant increase of elastic modulus and a constant decrease of elongation at break. Saravari *et al.* [12] observed a similar behavior with the parts produced through injection moulding using the composite of PP/ethylene octane copolymer (EOC)/wollastonite. While the increase in elongation at break was attributed to EOC, in a dose dependent manner, the filling with wollastonite having a high stiffness of 303 GPa could reduce the tensile strength while increasing tensile modulus due its restraining effect on the mobility of polymer chains. Despite the recorded low elongation at break of less than 1% of the test pieces, the current study found that the effect of the wollastonite filler on elastic modulus when added to CP75 PP for LS process is in agreement with the results obtained in cases of injection moulding. The presence of wollastonite in form of white particles as shown in the SEM image (Figure 3) contributed to enhancement of the tensile modulus up to 2308 MPa for test pieces built in x-direction.

3.2. Surface roughness

Surface texture plays a vital role in the functionality of mechanical components. Leach [3] reported that it is estimated that surface defects cause up to 10% of manufactured parts to fail. With respect to additive manufacturing (AM), this value is expected to be even higher due to the general poor surface finish of AM parts. Measurements of the surface finish of test blocks were performed using a Mitutoyo SURFTEST SJ-210 surface roughness tester. Surface roughness was measured on the up-facing horizontal surface of the blocks (Figure 4) produced in the x-direction with various scanning speeds. Figure 4 shows the results of the surface finish measurements.

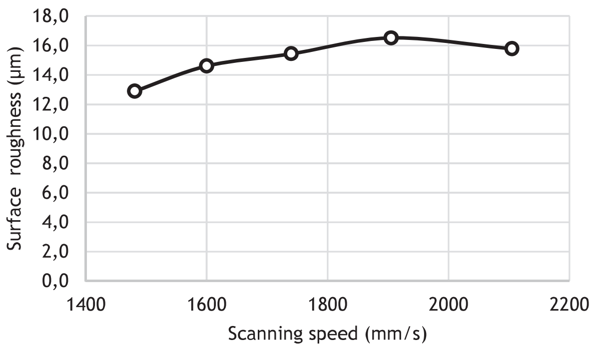

Figure 4: Scanning speed versus surface roughness

The surface finish was found to become gradually rougher as the scanning speed was increased. The variation of surface finish from 12 to 16 µm is not very significant within the range of scanning speeds that was investigated. This range can also be considered acceptable for polymer parts manufactured through LS.

3.3. Dimensional accuracy

Using an electronic Vernier caliper model KENNEDY® KEN-331-2320K with an accuracy of 0.01 mm, the dimensional accuracy of the block (Figure 1b) was assessed on the following geometrical features:

- The overall top dimensions 25 X 25 mm^2 of the block in x and y directions surface within accuracy of ±5%

- The height of 3 mm between a downskin surface and the top surface with accuracy of ±10%
- The height of 3 mm between an upskin surface and the bottom surface with accuracy of ±10%
- The thickness of two vertical walls of thickness of 1 mm and 0.75 mm with an accuracy of ±16%
- The quality of the inscribed texts on the part

3.3.1. The overall top dimensions 25X25 mm^2

Figures 5a and 5b show the deviations from the nominal dimension of 25 mm for x and y directions.

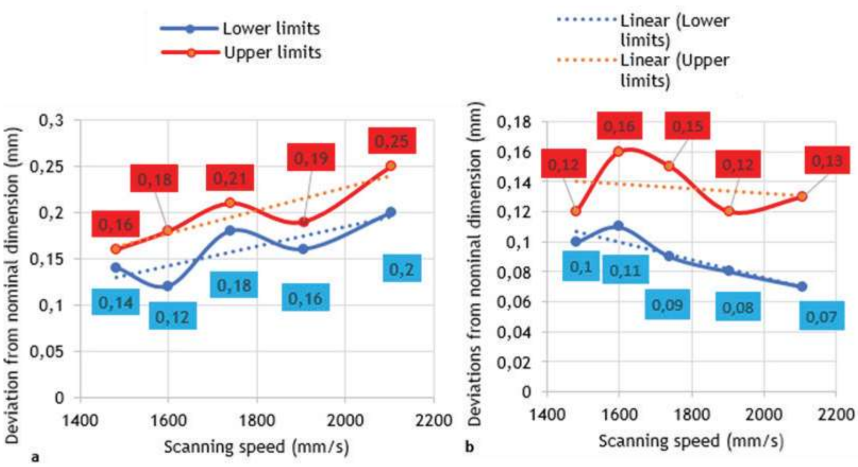

Figure 5: Dimensional deviations from 25 mm length in x-direction (a) and y-direction (b)

It was desirable to target an accuracy of ±5% for a length of 25 mm meaning that the lower and higher limits were expected to be 23.75 and 26.25 mm respectively. The measured values fall within 24.88 and 26.25 mm. From Figure 5, it can be observed that for all considered scanning speeds, the size of 25 mm in x direction satisfied the targeted accuracy, and the recorded measurements are between 25.12 and 25.25 mm for x-direction and 25.07 and 25.16 mm for y direction. The scaling factor of 1.019 in x, y and z directions led to all tolerances located on the positive side. Results show that tolerances are higher in x-direction compared to tolerances obtained in y-direction.

3.3.2. Upskin and downskin

In AM technology, the downfacing and upfacing surfaces are also known as the downskin and upskin surfaces respectively. The downskin and upskin surfaces always exist with parts containing holes or windows. As the part is supported by the powder during the building process, the downskin and upskin layers are in contact with the powder. The energy density input into the powder can influence the dimensions connected to the downskin and upskin layers. The accuracy of the build can be assessed by evaluation of the deviations from the nominal dimensions of the solid part of the component ending with the downskin or upskin layers. The results of measurement of the heights associated with the upskin and downskin surfaces are shown on Figure 6a and 6b.

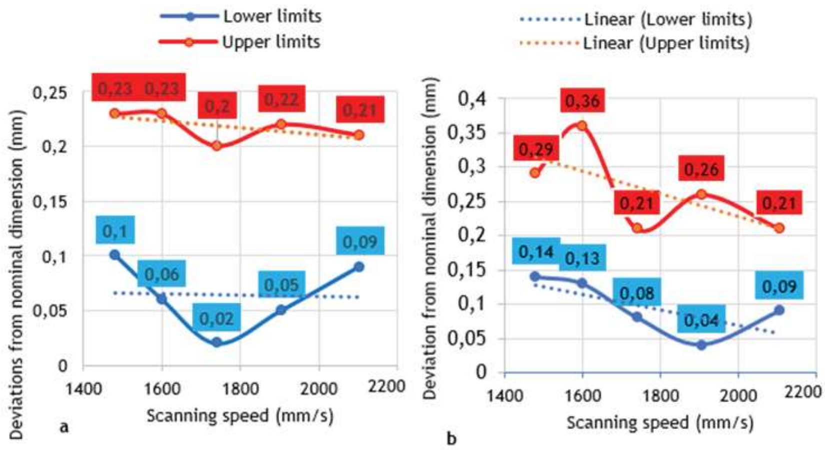

Figure 6: Dimensional deviation from 3 mm height measured to upskin (a) and to downskin (b)

All lower and upper deviations are on the positive side. The trendline of the measurements for the upskin surface show that the scanning speed has little influence on the upper and lower deviations from the nominal dimension. For the downskin surface, it can be observed that the trendlines show that the deviation decreases with an increase of the scanning speed. However, within the fixed dimensional accuracy of ±10%, all investigated scanning speeds for both upskin and down skin surfaces produced dimensions that fall within the acceptable range of 2.70 and 3.30 mm. For a given window, the upskin layer which later will support the powder is produced first, whereas the downskin layer supported by the powder is lastly added. The upskin experiences more time for consolidation compared to the downskin layer. The time difference for exposure to the heat and interaction with the powder may be the cause of the difference in the behavior in regards with the deviations from the nominal dimensions of the heights that are associated with the upskin and downskin layers.

3.3.3. Thin walls

Parts manufactured through LS process are exposed to very high temperatures throughout the build and are consequently susceptible to warping during the heating and cooling of each layer. Thinner walls are more likely to warp as they are subjected to heat and the weight of the powder with each consecutive layer. The accuracy of the wall thickness is a fundamental criterion to ensure the reliability of a LS process. Using a beam offset of 0.279 mm, layer thickness of 0.1 mm and a laser spot diameter of 0.47 mm for both x and y direction, Stratasys® Direct

Manufacturing, Inc. [13] investigated the success of formation of nylon 12 laser sintered small features such as wall thickness, holes, texts and movable components. When oriented vertically, walls thinner than 0.5 mm failed to form, while when oriented horizontally, walls with 0.5 mm thickness formed with significant warping. It was concluded that, regardless of orientation, reliable walls thinner than 0.5 mm are not accurately feasible. They recommended a minimum wall thickness of 0.8 mm to ensure rigidity of the feature. The resolution of horizontal walls is limited by the layer thickness while the resolution of the vertical walls is limited by the laser spot size. A better resolution in the horizontal direction was explained by the fact that the layer thickness was smaller than the laser spot size.

The dimensional accuracy of two vertical thin walls of thicknesses 0.75 and 1 mm on the test part in the current study was investigated. The results of measurement of thicknesses are shown on Figures 7a & b.

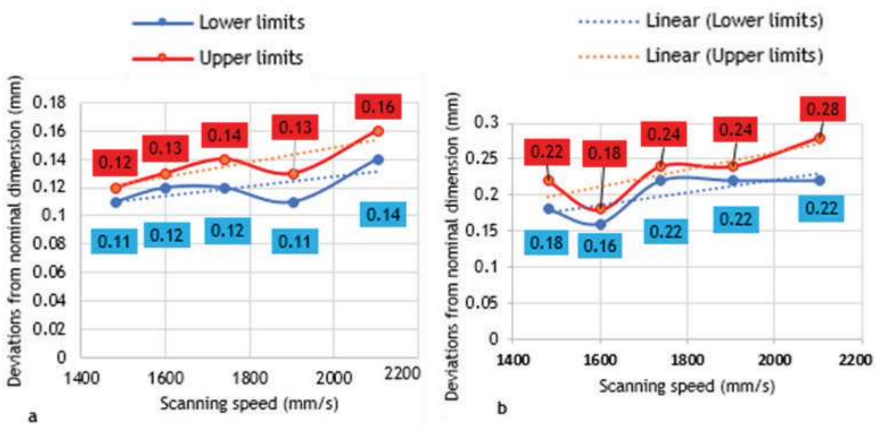

Figure 7: Dimensional deviations from a thin wall for thickness 0.75 mm (a) and 1 mm (b)

Similar to the above investigated dimensions, the lower and upper deviations from the nominal size of the thin walls are all in the positive direction. A visual inspection showed that the two thin walls were accurately formed though manually easy to break. The trendlines show that, for both thin walls, the lower and upper deviations from the nominal thickness increase with the increase of the scanning speed. For all considered scanning speeds, the wall of 0.75 mm of thickness failed to fall within 0.63 and 0.87 mm while for the thicker wall of 1 mm thickness, the full range of scanning speeds produced wall thicknesses that are within the acceptable limits of 0.84 and 1.16 mm. For the same scanning speed, the thinner wall of 0.75 mm thickness experiences higher deviations than the thicker wall of 1 mm thickness. It can be concluded that for the formation of walls thinner than 0.75 mm, a scanning speed of less than 1481 mm/s is required.

3.3.4. Texts inscribed on the part

To understand the quality of printing of the aesthetic features with the new PP powder, various texts were purposely designed on the test block or designed for identification of the build orientation and the associated process parameters. Table 2 summarizes the types, fonts, sizes and depths of the printed texts.

Table 2: Investigated quality texts

Texts	Font	Size (mm)	Depth (mm)	Purpose	Visual quality inspection
X and Y	Arial rounded MT	10	1.5	Text quality	Very good for all positions
Calibrate	Arial rounded MT	10	1.5	Text quality	Very good for all positions
1, 2 and 3	Arial rounded MT	10	1.5	Text quality	Very good for all positions
1	Century gothic	3.5	1.5	Text quality	Very good for all positions
mm	Century gothic	3.5	1.5	Text quality	Very good for all positions
.75	Arial	3.5	1.5	Text quality	Very good for all positions
+2, +1, 0, -2, -2, X, Y and Z	Arial	9.5	1	Process identification	Very good for all positions

Figure 8 shows images of the quality of the printed texts on the calibration block. The images were taken using a Sony Cyber-shot DSC-HX300 digital camera.

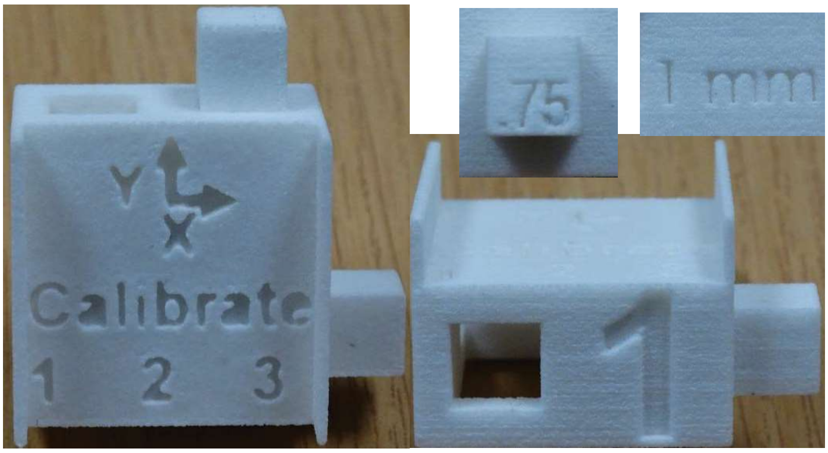

Figure 8: Quality of produced texts

A visual inspection could not establish a significant effect of the scanning speed on the quality of the texts printed on the pieces. Accurate texts with a very good readability were produced for all investigated texts fonts and sizes for all considered scanning speeds.

4. CONCLUSION

This study investigated the effect of scanning speed of parts produced through LS Diamond Plastics GmbH CP75 PP powder in terms of mechanical properties, dimensional accuracy and surface finish. Results showed that tensile strengths of 15.2, 12 and 7 MPa could be obtained in x, y and z-directions respectively for a scanning speed of 1600 mm/s. The tensile strength of test pieces produced in the x direction was therefore less than the 22 MPa claimed by the manufacturer of the powder. The highest moduli of elasticity of 2308 MPa in x and y directions and 1759 MPa in z-directions were obtained for a scanning speed of 1740 mm/s. However, a very low elongation at break, less than 1%, could be achieved which is significantly less than the 10% claimed by the manufacturer of the powder. The surface roughness and the deviations from the nominal 25 mm in x-direction and deviations from nominal thicknesses on a test block produced, increased with the scanning speed. The deviations from nominal dimensions associated with the upskin and downskin surfaces showed either neutral or decreasing trend with increase of the scanning speed. The accuracy of formation of walls thinner than 0.75 mm requires scanning speed lower than 1481 mm/s. The quality of the text for all considered sizes and fonts was excellent for all scanning speeds. Towards the end of the current study, the authors found that the data sheet for CP75 PP was changed on the Diamond Plastics GmbH website [14]. The wollastonite filler material in the PP powder was replaced with glass spheres, tensile strength in x direction is specified as 12 MPa, tensile modulus is 1500 MPa and elongation at break is 15%. Future research can focus on what effect the glass sphere filler has on the mechanical properties of CP75 PP powder processed through LS and how this compares with the older powder with wollastonite filler.

5 ACKNOWLEDGEMENTS

The financial support from the South African Research Chairs Initiative of the Department of Science and Technology and National Research Foundation of South Africa (Grant № 97994) and the Collaborative Program in Additive Manufacturing (Contract № CSIR-NLC-CPAM-15-MOA-CUT-01) is gratefully acknowledged. Thanks also to the University of the Free State and Central University of Technology, Free State collaborative programme for funding support. Thanks lastly to the Product Development and Technology Station (PDTS) and the Centre of Rapid Prototyping and Manufacturing (CRPM) for technical support.

REFERENCES

[1] **Goodridge, R.D., Tuck, C.J. & Hague, R.J.M.** 2012. Laser Sintering of polyamides and other polymers, *Progress in Materials Science* 57(2), pp 229-267.

[2] **Saravanan, M. & Khalid, A.S.** 2014. A Study on the Process Plant Design for the Production of a polypropylene plant, *International Journal of Emerging Technology and Advanced Engineering* 4(8), pp 631-635.

[3] **Leach, R.**, 2011, Optical Measurement of Surface Topography (Berlin: Springer).

[4] **Kleijnen, R.G., Schmid, M. & Wegener, M.** 2016. Nucleation and impact modification of polypropylene laser sintering parts, *AIP Conference Proceedings* 1779(1), 21-25 September 2015, Craz, Austria.

[5] **Fiedler, L., Correa, L.O.G., Radusch, H.J., Wutzler, A. & Gerken, J.** 2007. Evaluation of polypropylene powder grades in consideration of laser sintering processability, Journal of Plastics Technology 3(4), pp.1-14.

[6] **Lexow, M.M. & Drummer, D.** 2016. New materials for SLS: The use of antistatic and flow agents, Journal of Powder Technology, 2016, pp 1-9.

[7] **Tan, W.S., Chua, C.K., Chong, T.H., Fane, A.G. &Jia, A.** 2016. 3D printing by selective laser sintering of polypropylene channel spacers for spiral wound membrane modules for water industry, *Virtual and Physical Prototyping* 11(3), pp 151-158.

[8] **Zhu, W., Yan, C., Shi, Y., Wen, S., Liu, J. & Shi, Y.** 2015. Investigation into mechanical and microstructural properties of polypropylene manufactured by selective laser sintering in comparison with injection moulding counterparts, *Material and Design* 82, pp 37-45.
[9] **Diamond Plastics GmbH** [n.d.] Laser PP CP75 white, Available from http://www.diamond-plastics.de//en/products/laser-pp-cp-75.http. [Accessed on 15 March 2016].
[10] **Liparoti, S., Speranza, V., Sorrentino, A.& Titomanlio, G.** 2017. Polypropylene injection molded samples: Effect of mold temperature under uneven thermal conditions, *Polymers* 9(585), pp 1-18.

[11] **Abdurashirov, T.T. & Ob'edkov, A.L.** 2001. Possibility of modifying the properties of polyethylene by filling with wollastonite, *International Polymer Science and Technology* 28(8), pp 81-83.

[12] **Saravari, O., Waipunya, H. & Chuayjuljit, S.** 2016. Effect of ethylene octene copolymer and ultra wollastonite on the properties and morphology of polypropylene -based composites, *Journal of Elastomers & Plastics*, pp 1-12.
[13] **Stratasys® Direct, Inc. 2015. From design lab:** An insider's guide to laser sintering, Available from https://www.stratasysdirect.com/-/media/files/direct/.../ls_white_paper_201601-(2).pdf. [Accessed on 26 August 2018].
[14] **Diamond Plastics GmbH** [n.d.] Laser PP CP75 white, Available from http://www.diamond-plastics.de/en/products/laser-pp-cp-75.html. [Accessed on 14 August 2019).